MNRAS **472,** 3637–3647 (2017)
Advance Access publication 2017 August 26
doi:10.1093/mnras/stx2201

The AMBRE project: chemical evolution models for the Milky Way thick and thin discs

V. Grisoni,[1★] E. Spitoni,[1] F. Matteucci,[1,2,3] A. Recio-Blanco,[4] P. de Laverny,[4] M. Hayden,[4] Ŝ. Mikolaitis[4,5] and C. C. Worley[6]

[1]*Dipartimento di Fisica, Sezione di Astronomia, Università di Trieste, via G.B. Tiepolo 11, I-34131 Trieste, Italy*
[2]*INAF – Osservatorio Astronomico di Trieste, via G.B. Tiepolo 11, I-34131 Trieste, Italy*
[3]*INFN – Sezione di Trieste, via Valerio 2, I-34134 Trieste, Italy*
[4]*Laboratoire Lagrange, Universitè Côte d'Azur, Observatoire de la Côte d'Azur, CNRS, Bd de l'Observatoire, CS 34229, F-06304 Nice Cedex 4, France*
[5]*Institute of Theoretical Physics and Astronomy, Vilnius University, Saulėtekio al. 3, 10257 Vilnius, Lithuania*
[6]*Institute of Astronomy, University of Cambridge, Madingley Road, Cambridge CB3 0HA, UK*

Accepted 2017 August 23. Received 2017 August 23; in original form 2017 June 7

ABSTRACT

We study the chemical evolution of the thick and thin discs of the Galaxy by comparing detailed chemical evolution models with recent data from the Archéologie avec Matisse Basée sur les aRchives de l'ESO project. The data suggest that the stars in the thick and thin discs form two distinct sequences with the thick disc stars showing higher [α/Fe] ratios. We adopt two different approaches to model the evolution of thick and thin discs. In particular, we adopt (i) a two-infall approach where the thick disc forms fast and before the thin disc and by means of a fast gas accretion episode, whereas the thin disc forms by means of a second accretion episode on a longer time-scale; (ii) a parallel approach, where the two discs form in parallel but at different rates. By comparing our model results with the observed [Mg/Fe] versus [Fe/H] and the metallicity distribution functions in the two Galactic components, we conclude that the parallel approach can account for a group of α-enhanced metal-rich stars present in the data, whereas the two-infall approach cannot explain these stars unless they are the result of stellar migration. In both approaches, the thick disc has formed on a time-scale of accretion of 0.1 Gyr, whereas the thin disc formed on a time-scale of 7 Gyr in the solar region. In the two-infall approach, a gap in star formation between the thick and thin disc formation of several hundreds of Myr should be present, at variance with the parallel approach where no gap is present.

Key words: Galaxy: abundances – Galaxy: evolution – Galaxy: formation.

1 INTRODUCTION

In recent years, many spectroscopic surveys and projects have been developed in order to study the formation and evolution of the Milky Way, such as for example *Gaia*-ESO (Gilmore et al. 2012), APOGEE (Majewski et al. 2017) and the Archéologie avec Matisse Basée sur les aRchives de l'ESO (AMBRE) project (de Laverny et al. 2013). Furthermore, the arrival of *Gaia* data is enhancing the value of these surveys. For instance, the *Gaia*/Radial Velocity Spectrometer data will provide abundances data for several tenths of millions of stars (Recio-Blanco et al. 2016).

In this way, detailed stellar abundances of stars in the Milky Way can be measured. In particular, the latest observational data reveal a clear distinction between the abundance patterns of the thick and thin disc stars, especially for the α-elements. In fact, *Gaia*-ESO data (Recio-Blanco et al. 2014; Rojas-Arriagada et al. 2017), APOGEE data (Hayden et al. 2015) and AMBRE data (Mikolaitis et al. 2017) indicate two distinct sequences corresponding to thick and thin disc stars, and the presence of these two sequences still has to be interpreted in terms of Galactic chemical evolution models.

As pointed out in Matteucci (2012), Galactic chemical evolution models have passed through different phases that can be summarized as follows: (i) serial approach (e.g. Matteucci & Francois 1989); (ii) parallel approach (e.g. Ferrini et al. 1992; Pardi, Ferrini & Matteucci 1995; Chiappini 2009); (iii) two-infall approach (e.g. Chiappini, Matteucci & Gratton 1997; Romano et al. 2010); (iv) stochastic approach (e.g. Argast et al. 2000; Cescutti 2008).

In the serial approach, one assumes that the halo, thick and thin disc form in sequence. In this framework, the thick disc is simply a later phase relative to the halo and the thin disc is a later phase relative to the thick disc. In the parallel approach, the various Galactic stellar components start forming at the same time but evolve in parallel at different rates. The two-infall model belongs to the serial approach, but it assumes that the halo-thick disc formed out of a completely independent gas accretion episode relative to the thin disc. This latter formed out of different extragalactic gas on a much

★ E-mail: grisoni@oats.inaf.it

longer time-scale. In the stochastic approach, the early phases of the evolution are characterized by inhomogeneities of the interstellar medium (ISM), in the sense that the early supernovae (SNe) pollute only nearby regions and the mixing is not efficient.

In this paper, we will model the thick and thin disc evolution by adopting both the two-infall and the parallel approach.

The parallel approach was first introduced by Ferrini et al. (1992) and Pardi et al. (1995). In their model, they consider the three phases (halo, thick and thin discs) to evolve separately and in parallel. However, a limitation of this model is that the three phases are connected to one another through the infalling gas, and this fact prevents one to obtain a good agreement with the stellar metallicity distribution functions (MDFs) in the three phases. In fact, the three observed MDFs are different, indicating that each component cannot have formed out of gas shed by the other two (see Matteucci 2001). An advantage of their approach is that they can explain the observed spread in the data and the observed overlapping in metallicity of stars belonging to different components. A more recent parallel approach was suggested by Chiappini (2009) and Anders et al. (2017). The main difference between Chiappini (2009) and Pardi et al. (1995) is that in Chiappini's approach the thick and thin disc evolutions are completely disentangled.

On the other hand, the two-infall approach assumes two main infall episodes: during the first one, the halo-thick disc formed, whereas the second one gave rise to the thin disc. On this line, Chang et al. (1999) applied the two-infall model of Chiappini et al. (1997) to the thick and thin discs, although the data at that time were much less and sparse. In the original two-infall model, the thick disc was assumed to form fast on a time-scale no longer than 2 Gyr and it was considered together with the halo. Micali, Matteucci & Romano (2013) extended the two-infall model into a three-infall model where the formation of the thick disc was assumed to have occurred by means of a gas accretion episode totally independent from the episodes forming the halo and the thin disc. In their model, the thick disc formed faster than the thin disc and on a time-scale of 1 Gyr. They were able to reproduce the stellar MDFs of the thick and thin discs. However, for what concerns the [α/Fe] ratios, the available data were too sparse to identify different trends between the thick and thin disc stars. Recently, on the basis of the data of Adibekyan et al. (2012), Haywood et al. (2015) studied the evolution of the thick disc and concluded that the star formation history was uniform throughout the thick disc. They also concluded that the thick disc did not form inside out in the first 3–5 Gyr of the evolution of the Galaxy. Later on, Haywood et al. (2016) by considering APOGEE data concluded that there was a quenching in the star formation at the end of the thick phase. Kubryk, Prantzos & Athanassoula (2015) suggested instead that the thick disc is the result of stellar migration: they concluded that the thick disc is the early part of the Milky Way disc. They explained the sequences of [α/Fe] ratios of the thick and thin discs by analysing the data of Bensby, Feltzing & Oey (2014). Masseron & Gilmore (2015) by studying the APOGEE data concluded that the majority of thick disc stars formed earlier than the thin disc ones and that the star formation rate (SFR) in the thick disc was more efficient than in the thin disc.

The aim of this paper is to reproduce the chemical characteristics of the thick and thin disc stars as observed by the most recent data of the AMBRE project (Mikolaitis et al. 2017). The AMBRE abundances come from high-resolution (HR) data, similarly to those of Adibekyan et al. (2012), but they belong to a much larger sample. The AMBRE resolution is also higher than APOGEE data. In order to study these data, we test the two-infall and parallel scenarios, by means of improved and updated Galactic chemical evolution models. Our chemical models are based on the two-infall model (Chiappini et al. 1997; Romano et al. 2010) revisited and applied to the thick and thin discs and a new parallel model adopting two one-infall models for the thick and thin discs, respectively. In this way, the evolutions of the thick and thin discs are completely disentangled.

The paper is organized as follows. In Section 2, we present the data that have been used to make a comparison with the predictions of our chemical evolution models. In Section 3, we describe the chemical evolution models adopted. In Section 4, we show the comparison between model predictions and observations. Finally, Section 5 summarizes our results and conclusions.

2 OBSERVATIONAL DATA

The observational data used in this work for comparison with the chemical evolution models are issued from the AMBRE project (de Laverny et al. 2013). We recall that AMBRE has been defined in order to homogeneously determine stellar atmospheric parameters and chemical abundances for the archived spectra of the ESO spectrographs for Galactic archaeology purposes. Up to now, more than 200 000 HR spectra (including several repeats for several stars) have already been analysed. The corresponding atmospheric parameters have been derived thanks to the MATISSE algorithm (Recio-Blanco, Bijaoui & de Laverny 2006) and a large grid of FGKM synthetic spectra (de Laverny et al. 2012). In the present paper, we have adopted the magnesium and iron chemical abundances presented in Mikolaitis et al. (2017). These abundances have been derived owing to an automatic line-fitting technique for the AMBRE Fiber-fed Extended Range Optical Spectrograph and High Accuracy Radial velocity Planet Searcher spectra, which have been previously parametrized by Worley et al. (2012) and de Pascale et al. (2014), respectively. We also point out that the AMBRE sample is not complete and is characterized by different observational biases inherent to the content of the ESO archive. The present sample consists of 4666 individual slow-rotating stars, most of them ($\sim$11 per cent) being dwarfs of the solar neighbourhood for which accurate Mg and Fe are available. All of these targets have been classified owing to their Mg and Fe properties into five different Galactic components (thin and thick discs, metal-poor high/low α, and metal-rich high α, MRHA hereafter). We recall that it has been possible to conduct such a chemical labelling thanks to the small uncertainties of the derived abundances and also because magnesium is one of the best specy to separate the two Galactic discs (Mikolaitis et al. 2014).

Finally, we have recently analysed the kinematical and dynamical properties of the stars in the AMBRE catalogue (Hayden et al., in preparation). Those stars are also part of the TGAS catalogue (*Gaia* Collaboration, Brown et al. 2016b; Lindegren et al. 2016) included in the first data release of the *Gaia* mission (*Gaia* Collaboration, Prusti et al. 2016a). Thanks to the *Gaia* precise astrometry, we have been able to derive reliable orbital parameters for the stars using the GALPY code (Bovy 2015). In particular, the perigalacticon points of the orbits, derived by Hayden et al. (private communication), will be used in this paper.

3 THE MODELS

The chemical evolution models adopted here are

(i) the two-infall model (Chiappini et al. 1997; Romano et al. 2010) revisited and applied to the thick and thin discs, and

(ii) a new parallel model adopting two one-infall models for the thick and thin discs, respectively.

3.1 The two-infall model

The two-infall model adopted here is a revision of the model developed by Chiappini et al. (1997) and Romano et al. (2010). This model assumes that the Galaxy forms as a result of two main infall episodes. During the first one, the thick disc formed, whereas during the second one a much slower infall of gas, delayed with respect to the first one, gives rise to the thin disc. Here, we do not take into account the evolution of the halo, but we focus on the evolution of the thick and thin discs. The origin of the gas in the infall episodes is extragalactic and its composition is assumed to be primordial. The Galactic thin disc is approximated by several independent rings, 2 kpc wide, without exchange of matter between them whereas the evolution of the thick disc is fixed with radius.

The basic equations that describe the time evolution of G_i, namely the mass fraction of the element i in the gas, are (see Matteucci 2012)

$$\begin{aligned}\dot{G}_i(r,t) = &-\psi(r,t)X_i(r,t)\\ &+\int_{M_L(t)}^{M_{\rm Bm}}\psi(r,t-\tau_m)Q_{mi}(t-\tau_m)\phi(m)\mathrm{d}m\\ &+A\int_{M_{\rm Bm}}^{M_{\rm BM}}\phi(m)\cdot\left[\int_{\mu_m}^{0.5}f(\mu)\psi(r,t-\tau_{m2})Q_{mi}(t-\tau_{m2})\mathrm{d}\mu\right]\mathrm{d}m\\ &+(1-A)\int_{M_{\rm Bm}}^{M_{\rm BM}}\psi(r,t-\tau_m)Q_{mi}(t-\tau_m)\phi(m)\mathrm{d}m\\ &+\int_{M_{\rm BM}}^{M_U}\psi(r,t-\tau_m)Q_{mi}(t-\tau_m)\phi(m)\mathrm{d}m\\ &+\dot{G}_i(r,t)_{\rm inf}. \end{aligned}\quad (1)$$

As described in Matteucci (2012), the first term on the right-hand side of equation (1) represents the rate at which the chemical elements are subtracted from the ISM to be included into stars, whereas the various integrals represent the rate of restitution of matter from the stars into the ISM. In particular,

(i) The first integral represents the material restored by stars in the mass range $M_L(t)$–$M_{\rm Bm}$, where $M_L(t)$ is the minimum mass dying at the time t and its minimum value is $\simeq$0.8 $\mathrm{M}_\odot$ with a lifetime corresponding to the age of the Universe. The stellar lifetime of a star of mass m is defined as τ_m, and τ_{m_2} is the lifetime of the secondary star of those binary systems giving rise to SNe Ia (see the next). In fact, the clock to the explosion of these systems is given by the lifetime of the secondary star in the single-degenerate model (Matteucci & Greggio 1986). The term Q_{mi} is the new and already present fraction of an element i that is restored into the ISM by a star of mass m.

(ii) The second integral corresponds to the contribution of SNe Ia, as first introduced by Matteucci & Greggio (1986). Here, the rate is calculated by assuming the single-degenerate model for the progenitor of these SNe, namely a C-O WD plus a red giant companion. The extremes of this integral correspond to the minimum mass $M_{\rm Bm}$ and the maximum mass $M_{\rm BM}$ allowed for the whole binary systems giving rise to SNe Ia. The minimum mass $M_{\rm Bm}$ is set equal to 3 $\mathrm{M}_\odot$, in order to ensure that both the primary and the secondary star would be massive enough to allow the WD to reach the Chandrasekhar mass $M_{\rm Ch}$, after accretion from the companion. The maximum mass is fixed by the requirement that the mass of each component cannot exceed $M_{\rm up} = 8\,\mathrm{M}_\odot$, which is the assumed maximum mass giving rise to a C-O WD, and so $M_{\rm BM} = 16\,\mathrm{M}_\odot$. The function $f(\mu_B)$ describes the distribution of the mass ratio of the secondary of the binary system ($\mu_B = \frac{M_2}{M_B}$). The parameter A represents the fraction of binary systems with the right properties to give rise to SNe Ia, and it is assumed that $A = 0.035$. The time τ_{m2} is the lifetime of the secondary star in the binary system giving rise to an SN Ia, and represents the clock of the system in the single-degenerate scenario. In Matteucci et al. (2009), it has been demonstrated that this scenario is equivalent to the double-degenerate one as the effects on Galactic chemicevolution are concerned.

(iii) The third integral refers to single stars with masses in the range $M_{\rm Bm}$–$M_{\rm BM}$ (namely, 3–16 $\mathrm{M}_\odot$). They can be either stars ending their lives as C-O WDs or as SNe II (those with $M > M_{\rm up}$, which is assumed to be 8 $\mathrm{M}_\odot$).

(iv) The fourth integral represents the material restored by core-collapse SNe.

The last term in the equation is the gas accretion rate. In particular, the gas infall law is described as

$$\dot{G}_i(r,t)_{\rm inf} = A(r)(X_i)_{\rm inf}\mathrm{e}^{-\frac{t}{\tau_1}} + B(r)(X_i)_{\rm inf}\mathrm{e}^{-\frac{t-t_{\rm max}}{\tau_2}}, \quad (2)$$

where $G_i(r,t)_{\rm inf}$ is the infalling material in the form of element i and $(X_i)_{\rm inf}$ is the composition of the infalling gas that is assumed to be primordial. The parameter $t_{\rm max}$ is the time for the maximum mass accretion on to the disc and roughly corresponds to the end of the thick disc phase. The parameters τ_1 and τ_2 are the time-scales for mass accretion in the thick and thin disc components, respectively: they are the e-folding times of the mass accretion law and represent the times at which each component accumulated roughly half of its mass. These time-scales are free parameters of the model, and they are constrained mainly by comparison with the observed metallicity distribution of long-lived stars in the solar vicinity. The quantities $A(r)$ and $B(r)$ are two parameters fixed by reproducing the present-time total surface mass density in the solar neighbourhood as taken from Nesti & Salucci (2013). In particular, this is equal to 65 $\mathrm{M}_\odot$ pc^{-2} for the thin disc and 6.5 $\mathrm{M}_\odot$ pc^{-2} for the thick disc. Other studies suggest slightly different values for the total local surface mass density (Bovy & Rix 2013; Zhang et al. 2013; McKee, Parravano & Hollenbach 2015): we also tested these values and found negligible difference in the results. What really matters here is the ratio between the total surface mass density of the thick and thin discs, which is considered to be 1:10.

The SFR is the Schmidt–Kennicutt law (Kennicutt 1998a):

$$\psi(r,t) = \nu\sigma^k_{\rm gas}(r,t), \quad (3)$$

where $\sigma_{\rm gas}$ is the surface gas density, k is the law index and ν is the star formation efficiency (i.e. the SFR per unit mass of gas). The star formation efficiency is assumed to become zero when the surface gas density goes below a critical threshold $\sigma_{\rm th}$ (Kennicutt 1998a,b; Martin & Kennicutt 2001).

The initial mass function (IMF) can be parametrized as a power law of the following kind:

$$\phi(m) = am^{-(1+x)}, \quad (4)$$

generally defined in the mass range of 0.1–100 $\mathrm{M}_\odot$, where a is the normalization constant derived by imposing that

$$\int_{0.1}^{100} m\phi(m)\mathrm{d}m = 1. \quad (5)$$

In particular, we adopt the Kroupa, Tout & Gilmore (1993) IMF that corresponds to

$$x = 0.3 \text{ for } M \leq 0.5\,\mathrm{M}_{\odot}$$
$$x = 1.2 \text{ for } 0.5 M_{\odot} < M \leq 1.0\,\mathrm{M}_{\odot}$$
$$x = 1.7 \text{ for } M > 1.0\,\mathrm{M}_{\odot}. \quad (6)$$

3.2 The parallel model

Secondly, we consider the possibility of abandoning a sequential scenario like the one of the two-infall, in favour of a picture that treats the thick disc and the thin disc stars as two truly distinct evolutionary phases, which start at the same time but evolve independently. In the light of these considerations, we develop two distinct one-infall models: one for the thick disc and the other for the thin disc.

As in the previous model, the material accreted by the Galactic discs comes mainly from extragalactic sources, and the basic equation is the same seen before, i.e. equation (1).

Since this model assumes two distinct infall episodes, the gas infall is described as

$$(\dot{G}_i(r,t)_{\mathrm{inf}})|_{\mathrm{thick}} = A(r)(X_i)_{\mathrm{inf}} \mathrm{e}^{-\frac{t}{\tau_1}}, \quad (7)$$

$$(\dot{G}_i(r,t)_{\mathrm{inf}})|_{\mathrm{thin}} = B(r)(X_i)_{\mathrm{inf}} \mathrm{e}^{-\frac{t}{\tau_2}}, \quad (8)$$

for the thick disc and for the thin disc, respectively. The quantities $A(r)$ and $B(r)$ and the parameters τ_1 and τ_2 have the same meaning as discussed for equation (2). Actually, the exponential form is similar to the case of the two-infall model, but the novelty introduced here concerns the fact that the infall rates of the thick and thin discs are now totally disentangled. In fact, as mentioned above, we want to treat the thick and the thin disc as two truly distinct evolutionary phases.

For the SFR and the IMF, the functional forms are the same of the two-infall model [equations (3) and (6), respectively].

3.3 Nucleosynthesis prescriptions

The nucleosynthesis prescriptions and the implementation of the yields in the model are fundamental ingredients for chemical evolution models. In this work, we adopt the same nucleosynthesis prescriptions of model 15 of Romano et al. (2010), where an exhaustive description of the adopted yields can be found.

For the computation of the stellar yields, one has to distinguish between different mass ranges as well as single stars versus binary systems:

(i) low- and intermediate-mass stars (0.8–8 $\mathrm{M}_{\odot}$), which are divided into single stars and binary systems that can give rise to SNe Ia,
(ii) massive stars (M > 8 $\mathrm{M}_{\odot}$).

Single stars in the mass range 0.8–8 $\mathrm{M}_{\odot}$ contribute to the Galactic chemical enrichment through planetary nebula ejection and quiescent mass-loss along the giant branch. They enrich the ISM mainly in He, C and N, but they can also produce some amounts of ^{7}Li, Na and s-process elements. For these stars, which end their lives as white dwarfs (WDs), the adopted nucleosynthesis prescriptions are from Karakas (2010).

SNe Ia are considered to originate from carbon deflagration in C-O WDs in binary systems. These stars contribute a substantial amount of iron (0.6 $\mathrm{M}_{\odot}$ per event) and non-negligible quantities of Si and S. They also contribute to other elements, such as O, C, Ne, Ca, Mg and Mn, but in negligible amounts with respect to the masses of such elements ejected by SNe II. The adopted nucleosynthesis prescriptions are from Iwamoto et al. (1999).

Massive stars with masses $M > 8\,\mathrm{M}_{\odot}$ are the progenitors of SNe II, Ib and Ic: if the explosion energies are much higher than 10^{51} erg, hypernova events can occur (SNe Ic). For these stars, the adopted nucleosynthesis prescriptions are from Kobayashi et al. (2006) for the following elements: Na, Mg, Al, Si, S, Ca, Sc, Ti, Cr, Mn, Co, Ni, Fe, Cu and Zn. As for the He and CNO elements, we consider the results of Geneva models for rotating massive stars (see Romano et al. 2010). However, for Mg that is the one relevant element in this study, we adopted yields multiplied by a factor 1.2 in order to obtain a better agreement with the data. It is well known, in fact, that Mg yields have been underestimated in many nucleosynthesis studies (see François et al. 2004 for a discussion of this point), and although the most recent ones have improved, the Mg production in massive stars is still underestimated.

4 RESULTS

Good models of Galactic chemical evolution should reproduce the majority of the observational features and also a number of observational constraints that is larger than the number of free parameters. In this work, the observational constraints considered are the following ones:

(i) abundance patterns of the most common chemical elements, in particular the [Mg/Fe] versus [Fe/H] abundance pattern recently observed by the AMBRE project;
(ii) MDF of long-lived stars belonging to the thick and thin disc components as recently observed by the AMBRE project;
(iii) solar abundances;
(iv) present-time SFR;
(v) present-time Type Ia and Type II SN rates.

Our best models have been selected after running several numerical simulations by varying the most important input parameters one at a time. The input parameters of the best models are summarized in Table 1. In the first column, we give the names of the models: 2IM corresponds to the two-infall model, whereas 1IMT and 1IMt correspond to the one-infall models for the thick and thin discs, respectively. In the second column, we show the adopted IMF. In the third and fourth columns, there are the star formation efficiencies for the thick and thin discs, respectively. In the fifth and sixth columns, we give the time-scales for mass accretion in the thick

Table 1. Input parameters for the best chemical evolution models. 2IM corresponds to the two-infall model, whereas 1IMT and 1IMt correspond to the one-infall models for the thick and thin discs, respectively. In the second column, we show the adopted initial mass function. In the third and fourth columns, there are the star formation efficiencies for the thick and thin discs, respectively. In the fifth and sixth columns, we give the time-scales for mass accretion in the thick and thin discs, respectively. Finally, in last column, we show the adopted threshold in the SFR.

Model	IMF	ν_1 (Gyr^{-1})	ν_2 (Gyr^{-1})	τ_1 (Gyr)	τ_2 (Gyr)	σ_{th} ($\mathrm{M}_{\odot}$ pc^{-2})
2IM	Kroupa	2	1	0.1	7	7
1IMT	Kroupa	2	–	0.1	–	–
1IMt	Kroupa	–	1	–	7	7

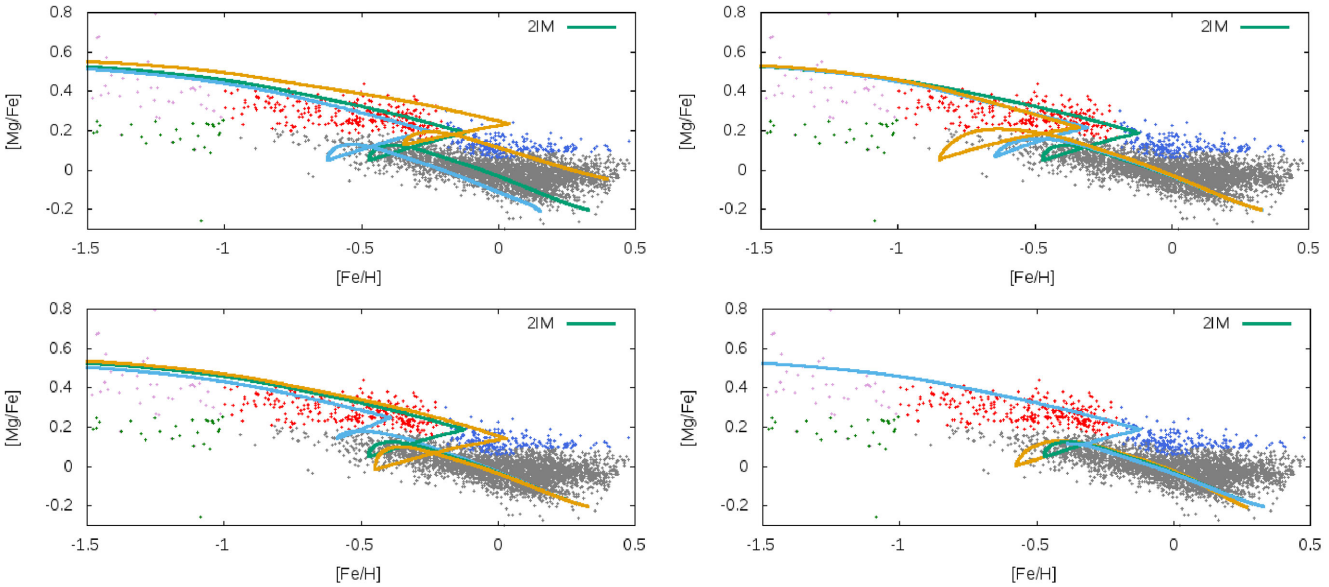

Figure 1. Predicted and observed [Mg/Fe] versus [Fe/H] in the solar neighbourhood in the case of the two-infall model. The data are from the AMBRE project and the different Galactic components are plotted: thin disc (grey dots), thick disc (red dots), MRHA sequence (blue dots), metal-poor low-α sequence (green dots), metal-poor high-α sequence (magenta). Upper-left panel: the effect of varying the IMF. The 2IM with Kroupa et al. (1993) IMF (green line) is compared with a model with Scalo (1986) IMF (light blue line) and Salpeter (1955) IMF (orange line). Lower-left panel: the effect of varying the star formation efficiency of the thick disc. The 2IM with $\nu_1 = 2$ Gyr^{-1} (green line) is compared with a model with $\nu_1 = 1$ Gyr^{-1} (light blue line) and $\nu_1 = 3$ Gyr^{-1} (orange line). Upper-right panel: the effect of varying the time-scale of the thick disc. The 2IM with $\tau_1 = 0.1$ Gyr (green line) is compared with a model with $\tau_1 = 0.5$ Gyr (light blue line) and $\tau_1 = 1$ Gyr (orange line). Lower-right panel: the effect of varying the threshold. The 2IM with $\sigma_{\rm th} = 7$ M$_\odot$ pc^{-2} (green line) is compared with a model with $\sigma_{\rm th} = 4$ M$_\odot$ pc^{-2} (light blue line) and $\sigma_{\rm th} = 10$ M$_\odot$ pc^{-2} (orange line).

and thin discs, respectively. Finally, in the last column, we show the adopted threshold in the SFR.

In Fig. 1, we show the effect of varying the most important input parameters of the two-infall model one at a time.

In the upper-left panel of Fig. 1, we show the effect of varying the IMF. We can see the prediction of the two-infall model in the solar vicinity for which we consider Kroupa et al. (1993) IMF, compared to the case with Scalo (1986) IMF and Salpeter (1955) IMF. We can see that Scalo (1986) IMF predicts too few massive stars, and so the corresponding track in the [Mg/Fe] versus [Fe/H] lies below the data. On the other hand, Salpeter (1955) IMF predicts too many massive stars, and so the corresponding track in the [Mg/Fe] versus [Fe/H] is above the data.

In the lower-left panel of Fig. 1, we show the effect of varying the star formation efficiency of the thick disc. We can see the prediction of the two-infall model in the solar vicinity for which the star formation efficiency of the thick disc is $\nu_1 = 1$, 2 and 3 Gyr^{-1}. We can see that a higher star formation efficiency implies a higher track in the [Mg/Fe] versus [Fe/H], even if the effect is less strong than in the case of varying the IMF. Furthermore, we can see that a higher star formation efficiency means a more rapid evolution for the thick disc, and this extends the range of [Mg/Fe] values for the thick disc stars.

In the upper-right panel of Fig. 1, we show the effect of varying the time-scale for mass accretion in the thick disc. We can see the prediction of the two-infall model in the solar vicinity for which the time-scale of the thick disc is $\tau_1 = 0.1$, 0.5 and 1 Gyr. We can see that a shorter time-scale for the thick disc formation extends the range of [Mg/Fe] values for the thick disc stars, because the evolution is more rapid.

In the lower-right panel of Fig. 1, we show the effect of varying the threshold in the SFR. We can see the prediction of the two-infall model in the solar vicinity for which the threshold is $\sigma_{\rm th} = 4$, 7 and 10 M$_\odot$ pc^{-2}. The gap in the model prediction is due to the assumed threshold in the star formation process. Varying the threshold means varying the extension of this gap, and the gap increases with increasing threshold.

On the other hand, the two parameters regarding the star formation efficiency and the time-scale for mass accretion in the thin disc are well constrained by reproducing the G-dwarf distribution and correspond to $\nu_2 = 1$ Gyr^{-1} and $\tau_2 = 7$ Gyr, as found in previous studies (Chiappini et al., 1997; Romano et al. 2010).

Similarly, we also chose the various input parameters for the one-infall models, as summarized in Table 1.

In the following, we focus on our best models and we show the predictions concerning the abundance patterns, the MDFs of the thick and thin discs, the solar abundances, the star formation history and the SN rates.

4.1 Abundance patterns

The first observational constraint considered is the [Mg/Fe] versus [Fe/H] relation, as observed by the AMBRE project.

In Fig. 2, we show the predicted and observed [Mg/Fe] versus [Fe/H] in the solar neighbourhood in the case of the two-infall model 2IM. The model predicts an overabundance of Mg relative to Fe to be almost constant until [Fe/H] < -1.5 dex, and then for [Fe/H] ~ -1.5 dex the trend shows a slight decrease due to the delayed explosion of SNe Ia. This behaviour of the abundance patterns of α-elements such as Mg is well interpreted in terms of the time-delay model (see Matteucci 2001, 2012): the time delay refers to the delay of iron ejection from SNe Ia relative to the faster production of α-elements by core-collapse SNe. The effect of the delayed iron production is to create an overabundance of α-elements

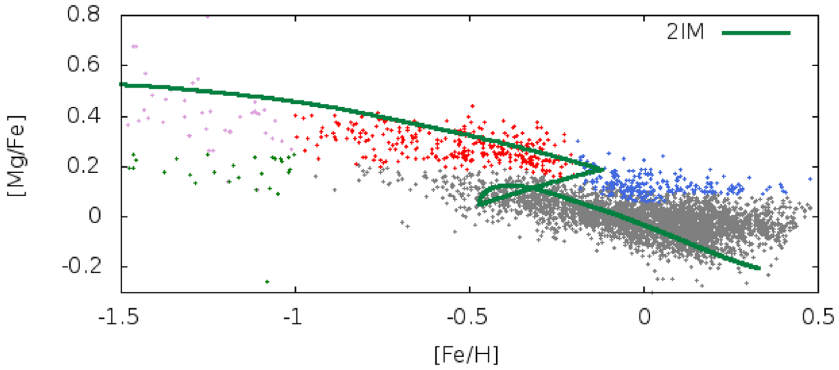

Figure 2. Predicted and observed [Mg/Fe] versus [Fe/H] in the solar neighbourhood in the case of the two-infall model. The data are from the AMBRE project and the different Galactic components are plotted: thin disc (grey dots), thick disc (red dots), MRHA sequence (blue dots), metal-poor low-α sequence (green dots), metal-poor high-α sequence (magenta). The predictions are from model 2IM (green line).

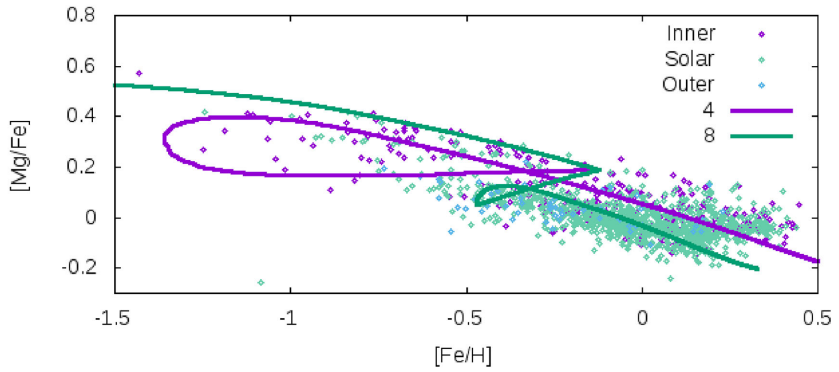

Figure 3. Predicted and observed [Mg/Fe] versus [Fe/H]. The data are colour-coded according to their guiding radius (inner, solar, outer) and the predictions are from model 2IM (both at 8 kpc and at 4 kpc).

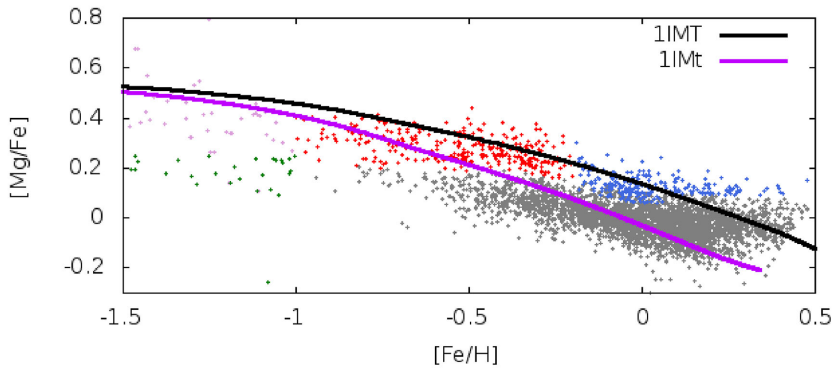

Figure 4. Same as Fig. 1, but the predictions are for models 1IMT for the thick disc (black line) and 1IMt for the thin disc (magenta line).

relative to iron at low [Fe/H] values, and a continuous decline of the [α/Fe] ratio until the solar value is reached. A peculiar feature of the 2IM is that at [Fe/H] ~ -0.2 dex we have a gap of 700 Myr duration due to the assumed threshold in the star formation process, which marks the transition between the thick and thin disc phases, where the star formation stops until the gas density in the thin disc reaches the threshold. A similar gap was found in the two-infall model of Chiappini et al. 1997), but between the halo-thick and thin disc phases, whereas here we focus on the disc (thick plus thin). It is worth noting that the 2IM model does not reproduce the metal-rich α-enhanced stars (MRHA, blue dots). If they are thick disc stars, this model cannot reproduce them since the thick disc does not extend far enough in [Fe/H]. However, these stars have shorter Rp (perigalacticon) values, and we could suppose that we see them now in the solar neighbourhood thanks to stellar migration from the inner thin disc.

In Fig. 3, we show the predictions of the 2IM also in a slice that is more internal than the solar neighbourhood, i.e. 4 kpc from the Galactic Centre. What differ from the 2IM for the solar neighbourhood are the time-scale of the thin disc (which is shorter and at 4 kpc is equal to 0.5 Gyr in the framework of an inside-out scenario) and the surface mass density (which changes with radius and at 4 kpc is equal to 303 $M_{\odot}$ pc^{-2} as in Nesti & Salucci 2013). According to the 2IM at 4 kpc, a large loop is evident in the abundance

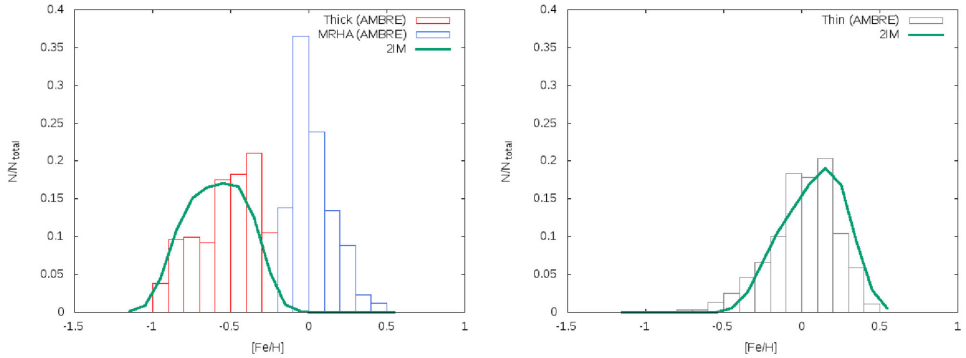

Figure 5. Left-hand panel:predicted and observed MDF of the thick disc in the case of the two-infall model. The data are from the AMBRE project: MDF of thick disc stars (red) and MDF of MRHA stars (blue). The predictions are from model 2IM (green line). We notice that the two-infall model cannot reproduce the MRHA stars, as explained in the text. Right-hand panel: predicted and observed MDF of the thin disc in the case of the two-infall model. The data are from the AMBRE project: MDF of thin disc stars (grey). The predictions are from model 2IM (green line).

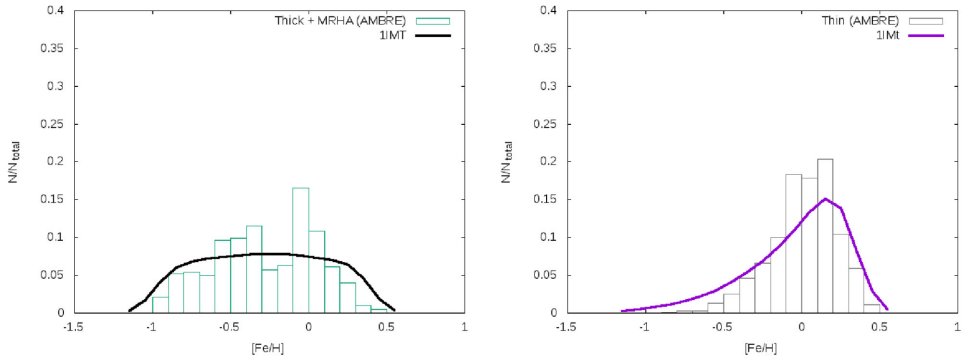

Figure 6. Same as Fig. 4, but the predictions are for models 1IMT for the thick disc (black line) and 1IMt for the thin disc (magenta line). We notice that in this case in the left-hand panel the MDF of thick plus MRHA stars is considered, since the one-infall model of the thick disc can also reproduce the MRHA stars.

pattern: this is due to the fact that the initial gas infall in the inner disc is more efficient than in the solar ring, and this produces a large [Fe/H] dilution between the thick and thin disc formation. In this case, the track in the abundance pattern is higher at higher metallicities and the MRHA stars can be fitted. Hence, these stars could be interpreted as stars that have migrated from the inner thin disc.

Then, in Fig. 4, we show the predicted and observed [Mg/Fe] versus [Fe/H] in the solar neighbourhood in the case of the parallel models 1IMT and 1IMt for the thick and thin discs, respectively. In the case of a parallel model, the thick and thin discs are treated as two truly distinct evolutionary phases and so we have two distinct tracks in the abundance pattern. Both the tracks show an overabundance of Mg relative to Fe to be almost constant until [Fe/H] < -1.5 dex, and then the trends show the decrease due to the delayed explosion of SNe Ia. However, the [α/Fe] ratios in the thick disc stars are higher than in the thin disc, as a consequence of the assumed faster evolution of the thick disc (a time-scale of the order of 0.1 Gyr, as shown in Table 1). Indeed, the fit to the data requires that the formation of the thick disc occur on shorter time-scales than the formation of the thin disc. In fact, a fast SFR and a short time-scale of gas accretion are required to form the thick disc, whereas a much slower SFR and longer accretion time-scale (7 Gyr, see Table 1) are necessary to reproduce the features of the thin disc. In Fig. 2, it is evident that with the parallel model we are able to reproduce the MRHA stars as metal-rich thick disc stars, since in the parallel approach the thick disc can extend up to high [Fe/H], at variance with the 2IM model.

4.2 Metallicity distribution functions

A fundamental constraint that we have to analyse is the MDF, both in the thick and thin discs. Thanks to our models, we are able to create two different MDFs, one for the thick and one for the thin disc.

First, let us consider the case of the two-infall model. Since the two-infall model predicts a gap in the star formation between the thick and thin discs, we consider as stars of the thick disc all those formed before the gap in the star formation and as stars of the thin disc all those formed afterwards.

(i) In the left-hand panel of Fig. 5, we show the predicted and observed MDF of the thick disc in the case of the two-infall model: the data are from the AMBRE project and the predictions are from model 2IM. From the data, we can see that the metallicity of the thick disc goes from [Fe/H] ~ -1.0 dex to [Fe/H] ~ -0.2 dex, and the mean value is $\langle$[Fe/H]$\rangle \sim -0.5$ dex. The 2IM well reproduces the observations. In fact, we have a tail of metal-poor stars and the same relative number for higher metallicity stars, and the relative number of stars with [Fe/H] ~ -0.5 dex predicted by the model is equal to $\sim$15 per cent. Therefore, as regard the thick disc, the model is good from the chemical point of view, as it predicts a relative number of stars in agreement with the observations, in the right [Fe/H] range. However, we notice that the 2IM model cannot reproduce the MRHA stars, because in the two-infall approach the thick disc phase does not extend so far in metallicity.

Table 2. Solar abundances (in dex).

Elem.	Observations	2IM	1IMt
O	8.66 ± 0.05	8.95	8.96
Mg	7.53 ± 0.09	7.58	7.59
Si	7.51 ± 0.04	7.71	7.72
S	7.14 ± 0.04	7.34	7.36
Fe	7.45 ± 0.05	7.64	7.66

(ii) In the right-hand panel of Fig. 5, we show the predicted and observed MDF of the thin disc in the case of the two-infall model: the data are from the AMBRE project and the predictions are from model 2IM. From the data, we can see that the metallicity of the thin disc goes from [Fe/H] ~ -0.5 dex to [Fe/H] ~ 0.5 dex, and the mean value is around the solar metallicity. Also in the case of the thin disc, the model is in good agreement with observations.

Secondly, let us consider the case of the parallel model.

(i) In the left-hand panel of Fig. 6, we show the predicted and observed MDF of the thick disc in the case of the parallel model: the data are from the AMBRE project and the predictions are from model 1IMT. To have a good agreement with the data, we have to consider the MDF of thick plus MRHA stars, which can be reproduced in the framework of the 1IMT model. In fact, the MDF predicted by model 1IMT is very broad and includes also the MRHA stars.

(ii) In the right-hand panel of Fig. 6, we show the predicted and observed MDF of the thin disc in the case of a parallel model: the data are from the AMBRE project and the predictions are from model 1IMt. Concerning the thin disc, the model is in quite good agreement with the data of the thin disc stars.

4.3 Solar abundances

In Table 2, the solar abundances predicted by the models 2IM and 1IMt are compared with observations of Grevesse, Asplund & Sauval (2007).

The abundances are expressed as $12 + \log(X/\mathrm{H})$. These abundances correspond to the composition of the ISM at the time of the formation of the Sun, 4.5 Gyr ago. Since we assume a Galactic lifetime of 13.7 Gyr, we have calculated the solar abundances at 9.2 Gyr after the big bang. Given the uncertainties, we can say that the predictions are in reasonable agreement with the observations. However, our predicted solar O is always a bit overestimated and the good agreement with the Mg solar abundance is due to the fact that we did increase the Mg yields from massive stars by multiplying them by a factor 1.2.

4.4 Star formation history

In Fig. 7, we show the SFR versus time as predicted by model 2IM. As we can see, the SFR is higher during the thick disc phase, while it is lower during the thin disc formation. A peculiar feature of this plot is the gap in the SFR between the thick disc and the thin disc formation. This is clearly due to the fact that the star formation in the thin disc occurs only after a density of 7 $\mathrm{M}_\odot\,\mathrm{pc}^{-2}$ has been accumulated. This gap was already predicted by Chiappini et al. (1997) for the 2IM model applied to the halo-thick disc and thin disc. The duration of the predicted gap between the thick and thin disc formation here is roughly 1 Gyr. An important constraint is represented by the present-time SFR in the solar vicinity, and

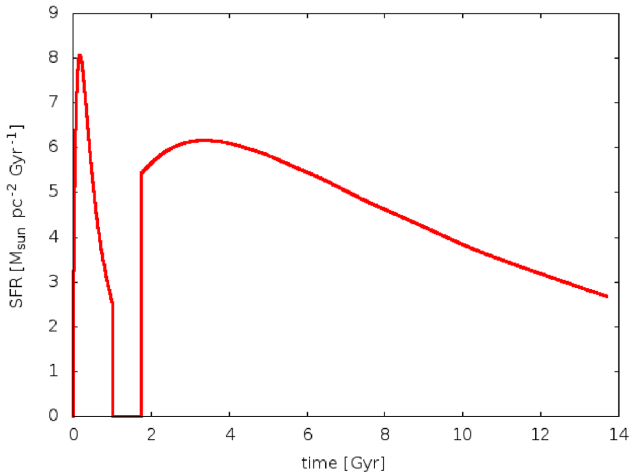

Figure 7. Temporal evolution of the SFR, as predicted by model 2IM.

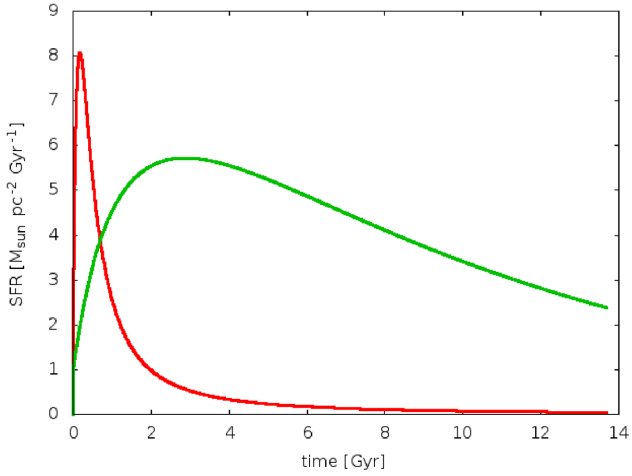

Figure 8. Temporal evolution of the SFR. Red line: prediction of model 1IMT. Green line: prediction of model 1IMt.

according to Bovy (2017) the present-time SFR as measured with *Gaia* is

$$\psi_0 \sim 1.7\,\mathrm{M}_\odot\,\mathrm{pc}^{-2}\,\mathrm{Gyr}^{-1},$$

with an e-folding time of ~7 Gyr. The value predicted by our best model is

$$\psi_0 = 2.7\,\mathrm{M}_\odot\,\mathrm{pc}^{-2}\,\mathrm{Gyr}^{-1},$$

in good agreement with observations.

In Fig. 8, we show the SFR versus time as predicted by models 1IMT and 1IMt for the thick and thin discs, respectively. The two SFRs are now separate, since we have assumed a distinct evolution for the two components of the disc, and there is no gap in star formation between the thick and thin disc phases. The star formation history of the thick disc is very different from the star formation history of the thin disc. In fact, the star formation history of the thick disc is peaked at earlier times, because it forms more rapidly than the thin disc (in fact, the thick disc has a higher star formation efficiency and a shorter time-scale of formation with respect to the thin disc). On the other hand, the SFR of the thin disc has a peak shifted to a later time and has still an active star formation at the

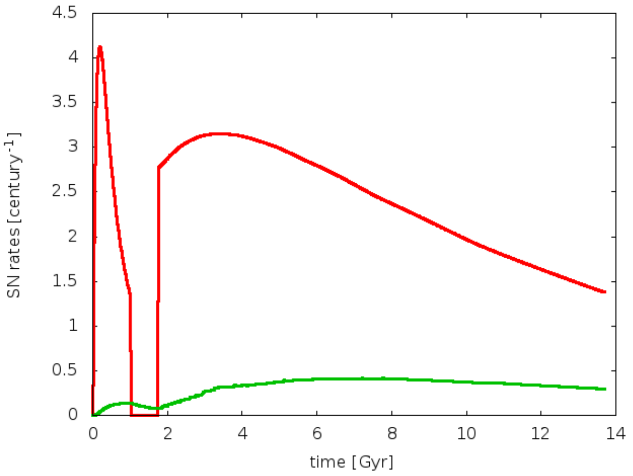

Figure 9. Temporal evolution of the SN rates, as predicted by model 2IM. Red line: SN II rates predicted by model 2IM. Green line: SN Ia rates predicted by model 2IM.

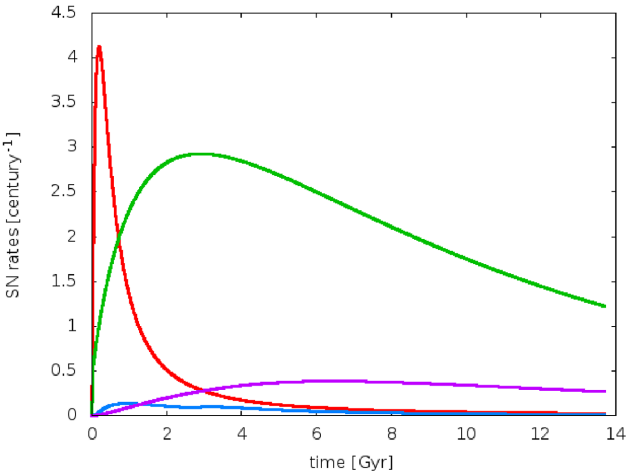

Figure 10. Temporal evolution of the SN rates. Red line: SN II rates predicted by model 1IMT. Green line: SN II rates predicted by model 1IMt. Blue line: SN Ia rates predicted by model 1IMT. Magenta line: SN Ia rates predicted by model 1IMt.

present time. The value predicted for the present-time SFR in the solar vicinity by model 1IMt is

$$\psi_0 = 2.4\,\mathrm{M}_\odot\,\mathrm{pc}^{-2}\,\mathrm{Gyr}^{-1},$$

also in this case, in agreement with observations. On the other hand, for the thick disc, there is no constraint available, since there is no active star formation at the present time.

4.5 SN rates

In Fig. 9, we show the predicted behaviour of the SN rates as a function of time as predicted by the two-infall model. As we can see, the gap between the end of the thick disc phase and the beginning of the thin disc phase, due to the adopted threshold, is also responsible for the trend of SN II rate. In fact, the trend shows a peak around ∼0.1 Gyr, which roughly corresponds to the time-scale of formation of the thick disc phase, and then goes to zero at a time of about 1 Gyr, which corresponds to the end of the thick disc phase. The explanation of this feature is that the SNe II originate from stars with high mass and short lifetime, and thus closely track the SFR and, hence, the number of this type of SNe per century is higher in the first gigayears of the formation of the Milky Way. Once the thick disc formation ends, star formation starts again and the number of SNe per century increases until 3 Gyr, and then decreases until the achievement of the present rate. On the other hand, the SNe Ia are produced by progenitors with long lifetimes; thus, they are very little influenced by the existence of a threshold in the star formation and the SN Ia rate increases with time and remains almost constant until the achievement of the present value. An important constraint is represented by the present-time SN rates in the solar vicinity, and according to Cappellaro & Turatto (1997), we have that

$$\mathrm{SNII} = 1.2 \pm 0.8\,\mathrm{century}^{-1},$$

$$\mathrm{SNIa} = 0.3 \pm 0.2\,\mathrm{century}^{-1},$$

or more recently according to Li et al. (2011):

$$\mathrm{SNCC} = 2.30 \pm 0.48\,\mathrm{century}^{-1},$$

$$\mathrm{SNII} = 1.54 \pm 0.32\,\mathrm{century}^{-1},$$

$$\mathrm{SNIa} = 0.54 \pm 0.12\,\mathrm{century}^{-1}.$$

The values predicted by the model 2IM are respectively

$$\mathrm{SNII} = 1.4\,\mathrm{century}^{-1},$$

$$\mathrm{SNIa} = 0.3\,\mathrm{century}^{-1},$$

in good agreement with observations.

On the other hand, in Fig. 10, we show the predicted behaviour of the SN rates as a function of time as predicted by the parallel model. The values of the present-time SN rates in the solar vicinity predicted by the 1IMt are

$$\mathrm{SNII} = 1.2\,\mathrm{century}^{-1},$$

$$\mathrm{SNIa} = 0.3\,\mathrm{century}^{-1},$$

also in this case, in agreement with observations.

5 CONCLUSIONS

In this work, we have studied the formation and evolution of the Milky Way thick and thin discs on the basis of detailed chemical evolution models to compare with the recent AMBRE [Mg/Fe] versus [Fe/H] (Mikolaitis et al. 2017).

In particular, we have explored two different approaches for modelling Galactic chemical evolution: the two-infall and the parallel approach. In the two-infall scenario, the Galaxy was formed by means of two infall episodes: during the first one, the thick disc formed whereas the second one gave rise to the thin disc. On the other hand, the parallel scenario assumes that the various Galactic components started forming at the same time but at different rates.

Our best models have been selected after performing several numerical simulations by varying the most important input parameters one at a time. The input parameters of the best models are $\tau_1 =$ 0.1 Gyr for the time-scale of formation of the thick disc and $\tau_2 =$ 7 Gyr for the time-scale of formation of the thin disc, $\nu_1 = 2\,\mathrm{Gyr}^{-1}$ for the star formation efficiency of the thick disc and $\nu_2 = 1\,\mathrm{Gyr}^{-1}$ for the star formation efficiency of the thin disc, $\sigma_{\mathrm{th}} = 7\,\mathrm{M}_\odot\,\mathrm{pc}^{-2}$

for the assumed threshold in the SFR, and a Kroupa et al. (1993) IMF.

Our conclusions are as follows.

(i) As regard the abundance patterns, we have focused on the α-element for which there is a clear distinction between thick and thin disc stars. The two-infall model can reproduce the thick and thin disc stars, but not the MRHA stars unless we assume that these stars have migrated from the inner thin disc. On the other hand, the parallel model treats the thick and thin discs as two truly distinct and parallel evolutionary phases and so we have two distinct tracks in the abundance pattern. With the parallel model, we are able to reproduce the MRHA stars as the metal-rich thick disc stars, since in the parallel approach the thick disc can extend up to high [Fe/H], at variance with the two-infall sequential model.

(ii) For the MDFs, the two-infall model can reproduce the MDF of the thick and thin disc stars, whereas it cannot reproduce the MRHA stars. On the other hand, with the parallel model the MDF of the thick disc is very broad and also includes the MRHA stars. We underline that the MDF represents a fundamental constraint for chemical evolution models because it is strongly dependent on the mechanism of disc formation. In particular, for our best models in the parallel scenario, the time-scale for the formation of the thick disc is equal to 0.1 Gyr, whereas the time-scale for the formation of the thin disc at solar position is much longer and it is equal to 7 Gyr. Both these time-scales are dictated by reproducing the MDF of each Galactic component.

(iii) Concerning the solar abundances, the predictions of all models are in reasonable agreement with the observations of Grevesse et al. (2007), but for Mg we had to increase the canonical yields from massive stars by a factor of 1.2.

(iv) The predicted present-time SFR is $\psi_0 = 2.7\,\mathrm{M}_\odot\,\mathrm{pc}^{-2}\,\mathrm{Gyr}^{-1}$ (for the two-infall model) and $\psi_0 = 2.4\,\mathrm{M}_\odot\,\mathrm{pc}^{-2}\,\mathrm{Gyr}^{-1}$ (for the one-infall model of the thin disc), both in good agreement with observations. The predicted present-time SN II rate is 1.4 century^{-1} (for the two-infall model) and 1.2 century^{-1} (for the one-infall model of the thin disc), whereas the predicted present-time SN Ia rate is 0.3 century^{-1} (for the two-infall model) and 0.3 century^{-1} (for the one-infall model of the thin disc), in good agreement with the observations.

(v) In the two-infall approach, there is a gap in star formation between the thick and thin disc formation of several hundreds of Myr ($\sim$700 Myr), at variance with the parallel approach where no gap is present.

To summarize, a sequential approach like the one of the two-infall model can reproduce the chemical properties of thick and thin disc stars, but not those of the MRHA stars. In this case, these stars can be explained only by stellar migration from the inner disc. On the other hand, in order to reproduce the chemical properties of the MRHA stars without invoking stellar migration, it is better to consider a parallel scenario where the evolutions of the thick and thin discs are separated. In this way, the MRHA stars can be interpreted as metal-rich thick disc stars. However, the nature of these MRHA stars is still uncertain, and forthcoming data concerning the ages of these stars will be fundamental to further constrain the disc formation and evolution.

ACKNOWLEDGEMENTS

This work has made use of data from the European Space Agency (ESA) mission *Gaia* (https://www.cosmos.esa.int/gaia), processed by the *Gaia* Data Processing and Analysis Consortium (DPAC, https://www.cosmos.esa.int/web/gaia/dpac/consortium). Funding for the DPAC has been provided by national institutions, in particular the institutions participating in the *Gaia* Multilateral Agreement.

FM, VG and ES acknowledge financial support from the University of Trieste (FRA2016). We also acknowledge useful discussions with A. Rojas-Arriagada.

Finally, we thank an anonymous referee for useful suggestions that improved the paper.

REFERENCES

Adibekyan V. Z., Sousa S. G., Santos N. C., Delgado Mena E., González Hernández J. I., Israelian G., Mayor M., Khachatryan G., 2012, A&A, 545, A32
Anders F. et al., 2017, A&A, 597, A30
Argast D., Samland M., Gerhard O. E., Thielemann F. K., 2000, A&A, 356, 873
Bensby T., Feltzing S., Oey M. S., 2014, A&A, 562, A71
Bovy J., 2015, ApJS, 216, 29
Bovy J., 2017, MNRAS, 470, 1360
Bovy J., Rix H. W., 2013, ApJ, 779, 115
Cappellaro E., Turatto M., 1997, in Ruiz-Lapuente P., Canal R., Isern J., eds, NATO Advanced Science Institutes (ASI) Ser. C, Vol. 486. Kluwer, Dordrecht, p. 77
Cescutti G., 2008, A&A, 481, 691
Chang R. X., Hou J. L., Shu C. G., Fu C. Q., 1999, A&A, 350, 38
Chiappini C., 2009, in Andersen J., Bland-Hawthorn J., Nordström B., eds, Proc. IAU Symp. 254, The Galaxy Disk in Cosmological Context. Cambridge Univ. Press, Cambridge, p. 191
Chiappini C., Matteucci F., Gratton R., 1997, ApJ, 477, 765
de Laverny P., Recio-Blanco A., Worley C. C., Plez B., 2012, A&A, 544, A126
de Laverny P., Recio-Blanco A., Worley C. C., De Pascale M., Hill V., Bijaoui A., 2013, The Messenger, 153, 18
De Pascale M., Worley C. C., de Laverny P., Recio-Blanco A., Hill V., Bijaoui A., 2014, A&A, 570, A68
Ferrini F., Matteucci F., Pardi C., Penco U., 1992, ApJ, 387, 138
François P., Matteucci F., Cayrel R., Spite M., Spite F., Chiappini C., 2004, A&A, 421, 613
Gaia Collaboration, Prusti T. et al., 2016a, A&A, 595, A1
Gaia Collaboration, Brown A. G. A. et al., 2016b, A&A, 595, A2
Gilmore G. et al., 2012, The Messenger, 147, 25
Grevesse N., Asplund M., Sauval A. J., 2007, Space Sci. Rev., 130, 105
Hayden M. R. et al., 2015, ApJ, 808, 132
Haywood M., Di Matteo P., Snaith O., Lehnert M. D., 2015, A&A, 579, A5
Haywood M., Lehnert M. D., Di Matteo P., Snaith O., Schultheis M., Katz D., Gómez A., 2016, A&A, 589, A66
Iwamoto K., Brachwitz F., Nomoto K., Kishimoto N., Umeda H., Hix W. R., Thielemann F. K., 1999, ApJS, 125, 439
Karakas A. I., 2010, MNRAS, 403, 1413
Kennicutt R. C., Jr, 1998a, ApJ, 498, 541
Kennicutt R. C., Jr, 1998b, ARA&A, 36, 189
Kobayashi C., Umeda H., Nomoto K., Tominaga N., Ohkubo T., 2006, ApJ, 653, 1145
Kroupa P., Tout C. A., Gilmore G., 1993, MNRAS, 262, 545
Kubryk M., Prantzos N., Athanassoula E., 2015, A&A, 580, A126
Li W., Chornock R., Leaman J., Filippenko A. V., Poznanski D., Wang X., Ganeshalingam M., Mannucci F., 2011, MNRAS, 412, 1473
Lindegren L. et al., 2016, A&A, 595, A4
McKee C. F., Parravano A., Hollenbach D. J., 2015, ApJ, 814, 13
Majewski S. R. et al., 2017, AJ, 154, 94
Martin C. L., Kennicutt R. C., Jr, 2001, ApJ, 555, 301
Masseron T., Gilmore G., 2015, MNRAS, 453, 1855
Matteucci F., 2001, in Astrophysics and Space Science Library, Vol. 253, The Chemical Evolution of the Galaxy. Kluwer, Dordrecht
Matteucci F., 2012, Chemical Evolution of Galaxies. Springer-Verlag, Berlin
Matteucci F., Francois P., 1989, MNRAS, 239, 885

Matteucci F., Greggio L., 1986, A&A, 154, 279
Matteucci F., Spitoni E., Recchi S., Valiante R., 2009, A&A, 501, 531
Micali A., Matteucci F., Romano D., 2013, MNRAS, 436, 1648
Mikolaitis Š. et al., 2014, A&A, 572, A33
Mikolaitis Š., de Laverny P., Recio-Blanco A., Hill V., Worley C. C., de Pascale M., 2017, A&A, 600, A22
Nesti F., Salucci P., 2013, J. Cosmol. Astropart. Phys., 7, 016
Pardi M. C., Ferrini F., Matteucci F., 1995, ApJ, 444, 207
Recio-Blanco A., Bijaoui A., de Laverny P., 2006, MNRAS, 370, 141
Recio-Blanco A. et al., 2014, A&A, 567, A5
Recio-Blanco A. et al., 2016, A&A, 585, A93
Rojas-Arriagada A. et al., 2017, A&A, 601, A140
Romano D., Karakas A. I., Tosi M., Matteucci F., 2010, A&A, 522, A32
Salpeter E. E., 1955, ApJ, 121, 161
Scalo J. M., 1986, Fundam. Cosm. Phys., 11, 1
Worley C. C., de Laverny P., Recio-Blanco A., Hill V., Bijaoui A., Ordenovic C., 2012, A&A, 542, A48
Zhang L., Rix H. W., van de Ven G., Bovy J., Liu C., Zhao G., 2013, ApJ, 772, 108

This paper has been typeset from a TEX/LATEX file prepared by the author.